Int. J. Electrochem. Sci., 17 **(2022)** Article Number: 220752, doi: 10.20964/2022.07.45

International Journal of
ELECTROCHEMICAL
SCIENCE
www.electrochemsci.org

Study on Zn-Ni Electrodeposited coating on 40Mn Steel as Construction Material and its Corrosion Resistance in Simulated Concrete Pore Solution

Yingguang Wang

Jilin Province Economic Management Cadre College, College of Architectural Engineering, China
Jilin, Changchun 130000
E-mail: wyg_college@yeah.net

Received: 15 March 2022 / *Accepted:* 8 May 2022 / *Published:* 6 June 2022

In this paper, Zn-Ni alloy coating is prepared on 40Mn steel as construction material by electrodeposition and the corrosion behavior of Zn-Ni alloy in simulated concrete pore solution is studied. It is found that the zinc content in Zn-Ni alloy coating is much higher than nickel content. Moreover, the amount of nickel in the Zn-Ni ally coating is much less than that of in the plating solution due to anomalous co-deposition. Appropriate current density is beneficial to accelerate the deposition rate of nickel, increase the current efficiency and improve the nickel content in the coating, so as to obtain strip grain structure with excellent corrosion resistance. When the current density reaches 3 A/dm^2, the content of nickel in the Zn-Ni alloy coating decreases and the corrosion resistance also decreases due to the intense hydrogen evolution and a large amount of metal hydroxide absorbed on the cathode surface. The surface morphology of Zn-Ni alloy coating obtained by 2.5 A/dm^2 is compact with 15.4% nickel and 23.4 μm thickness leading to the best corrosion resistance.

Keywords: Construction materials; Zn-Ni coating; Simulated concrete pore solution; Electrodeposition;

1. INTRODUCTION

Carbon steel is widely used in construction industry, especially in concrete field, because of its advantages of simple preparation process, low price and excellent mechanical performance [1-4]. However, the corrosion resistance of carbon steel is poor. In order to improve the corrosion resistance of carbon steel in concrete, zinc coating is usually prepared on carbon steel. Zinc coating on iron substrate is acted as anodic coating in general corrosive medium, which can protect the substrate to some extent [5-8]. But at high temperature, the electrode potential of metal zinc is more positive than that of metal iron, and it loses its protection for substrate. Moreover, corrosion resistance of zinc

coating in acid solution is very poor. Therefore, the traditional zinc layer cannot well protect the carbon steel in concrete from the concrete pore solution. It is found that zinc alloy prepared on carbon steel can effectively improve the corrosion resistance of carbon steel. The common feature of zinc alloys is that they have good corrosion resistance, which can effectively protect the substrate from corrosion. At present, a large number of zinc alloys with excellent corrosion resistance are reported, including Zn-Ni, Zn-Co, Zn-Fe and so on [9-13]. Among them, Zn-Ni alloy is widely concerned because of its low cost and simple preparation. The main methods for preparing Zn-Ni alloys are physical and chemical. Physical methods are rarely used in the construction industry due to their high cost and complex process. Chemical methods, especially electrochemical methods, have the advantages of simple process, low cost and controllable process, and are widely used to prepare Zn-Ni alloys. It is found that the content of nickel in Zn-Ni is closely related to its corrosion resistance. Zn-Ni electrodeposited coating belongs to anomolous co-deposition. Although nickel is easier to be deposited than zinc, zinc deposition in the actual electrodeposition process will hinder the electrodeposition process of nickel, resulting in a lower content of nickel in the coating. At present, studies have found that increasing the temperature, increasing the concentration of nickel salt or magnetic field assisted electrodeposition can effectively increase the content of nickel in Zn-Ni alloy, but the cost is high [14-16]. Since nickel belongs to electrochemical control, increasing current density can promote the deposition of nickel, which is beneficial to increase the content of nickel in Zn-Ni alloy. Therefore, Zn-Ni alloy is electrodeposited on the 40Mn steel as construction material to improve the corrosion resistance of 40Mn steel in simulated concrete pore solution. Moreover, the effect of current density on anomalous co-deposition process of Zn-Ni alloy is studied.

2. EXPERIMENTAL

The 40Mn steel plate (2 cm×3 cm×0.1 cm) is used as the substrate and the pure nickel plate (3 cm×5 cm×0.1 cm) is used as the anode in the experiment. The detail information about solution composition is listed in Table 1.

Table 1. Solution composition of Zn-Ni electrodeposited coating; All the chemical reagents are chemically pure mixed in the 100 ml aqueous solution.

Chemical reagent	Concentration (gL^{-1})
$ZnCl_2$	100
$NiCl_2$	50
KCl	120
NH_4Cl	30
H_3BO_3	35

Meanwhile, the zinc and nickel ions derive from the chemical reagent $ZnCl_2$ and $NiCl_2$. KCl is used as a conductivity salt, which can improve the conductivity of plating solution. Chloride ion is

very important during Zn-Ni electrodeposition process. A high coordination complex $K_4(ZnCl_6)$ will be formed if the concentration of chloride ion in the plating solution is higher than that of zinc ion which can help to increase cathodic polarization. The pH value of cathode will increase slowly during the electrodeposition process due to the hydrogen evolution. The H_3BO_3 is used as the buffer to adjust the pH value of plating solution. Pretreatment technology is necessary to remove oil and get rid of rust on the surface of substrate before Zn-Ni electrodeposition. The alkali solution with 30 g/L sodium hydroxide is used to remove oil on the substrate at 60 ℃ for 15 min. And then, the acid solution with 15% hydrochloric acid is used to clean the rust on the substrate at 30 ℃ for 5 min. Finally, the substrate is immersed into the plating solution composed of chemical agents listed in table 1 to electrodeposite Zn-Ni coating at 60 ℃ for 60 min. The current density is ranged from 1 A/dm^2 to 3 A/dm^2 to study the effect on the performance of Zn-Ni coatings. The schematic diagram of Zn-Ni electrodeposited coating is shown in figure 1.

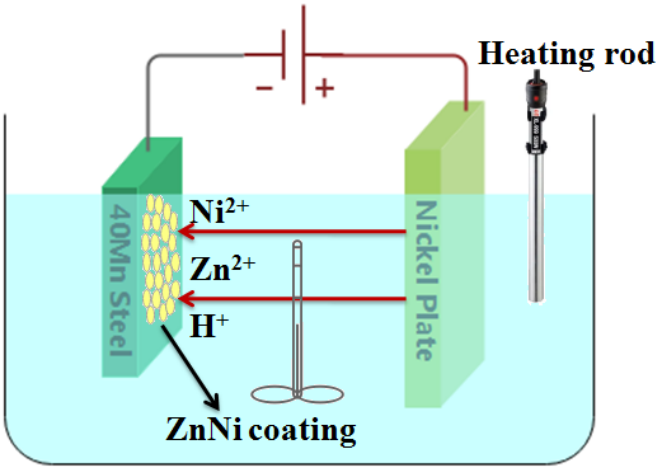

Figure 1. The schematic diagram of ZnNi coating electrodeposition; The 40Mn steel plate (2 cm×3 cm×0.1 cm) is used as the substrate and the pure nickel plate (3 cm×5 cm×0.1 cm) is used as the counter electrode in the experiment. The electrodeposition lasts for 60 min at 60 ℃.

After the Zn-Ni coating electrodeposition is finished, the Zn-Ni coating is clean and dried to do the performance testing. The cyclic voltammetry and chronoamperometry curves of Zn-Ni electrodeposition are tested by electrochemical station (PARSTAT 2273). The working electrode is 40Mn steel plate (1 cm×1 cm×0.1 cm) while the counter electrode is pure platinum plate (2 cm×2 cm×0.1 cm). The saturated calomel electrode is used as the reference electrode. The initial potential is set to 0 V. The most negative potential is -1.5 V while the most positive potential is 0.5 V with scanning rate 0.03 V/s in the different solutions containing 0.01 mol/L $NiCl_2$, 0.01 mol/L $ZnCl_2$ and 0.01 mol/L $NiCl_2$+$ZnCl_2$ respectively. The chronoamperometry curves of 40Mn steel plate in different plating solutions containing 0.01 mol/L $NiCl_2$, 0.01 mol/L $ZnCl_2$ and 0.01 mol/L $NiCl_2$+$ZnCl_2$ respectively keep at -1.3 V for 5 min. Thickness of the Zn-Ni coating is calculated by 3D surface profiler (Klatencor P7) and the composition of Zn-Ni coating is tested by EDX300B. Moreover, SEM (Hitachi TM3030) is used to observe the surface morphology of samples. Finally, the Zn-Ni coating is cut into 1 cm×1 cm×0.1 cm as the cathode. The pure platinum plate (2 cm×2 cm×0.1 cm) is as the anode. The saturated calomel electrode is chosen as the reference electrode. The polarization curve of

Zn-Ni coating in 100 ml simulated concrete pore solution (Table 2) is tested to evaluate the corrosion resistance.

Table 2. Chemical composition of simulated concrete pore solution; All the chemical reagents are chemically pure mixed in the 100 ml aqueous solution.

Chemical reagent	Concentration (gL^{-1})
$Ca(OH)_2$	2
NaCl	3

3. RESULT AND DISCUSSION

3.1 Cyclic voltammetry and chronoamperometry curves

Figure 2 shows the cyclic voltammetry curves of different plating solutions with zinc and nickel ions. According to figure 2, it is obvious that with the potential moves to negative position, the cathode current increases gradually.

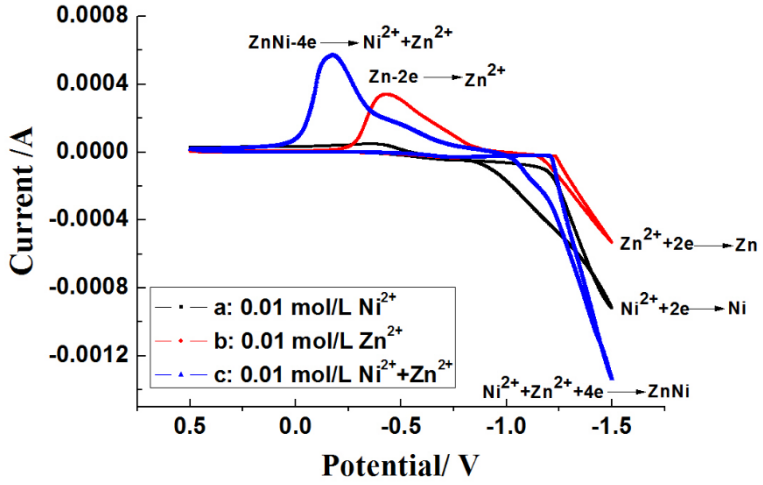

Figure 2. Cyclic voltemmetry curve of 40Mn steel plate in different plating solutions; a: 0.01 mol/L $NiCl_2$; b: 0.01 mol/L $ZnCl_2$; c: 0.01 mol/L $NiCl_2$+$ZnCl_2$; The working electrode is 40Mn steel plate (1 cm×1 cm×0.1 cm) while the counter electrode is pure platinum plate (2 cm×2 cm×0.1 cm). The saturated calomel electrode is used as the reference electrode. The initial potential is set to 0 V. The most negative potential is -1.5 V while the most positive potential is 0.5 V with scanning rate 0.03 V/s.

The cathode current of solution containing 0.01 mol/L zinc ions start to increase sharply at the position of -1.23 V while the cathode current of solution with 0.02 mol/L nickel ions begin to increase extremely at the position of -1.16 V which means that nickel is easier to be electrodeposited than zinc. However, the cathode current of mixed solution with 0.01 mol/L zinc ions and 0.01 mol/L nickel ions increases dramatically at the position of -1.20 V which shows that zinc ion in solution inhibits the

electrodeposition of nickel to a certain extent. According to the oxidation peak of the cyclic voltammetry curve, it can be found that the oxidation peak of nickel is near -0.37 V, while the oxidation peak of zinc is near -0.43V, indicating that nickel has better corrosion resistance than zinc. However, the oxidation peak of Zn-Ni alloy appears near -0.17 V. Compared with the oxidation peak of zinc and nickel, the oxidation peak of Zn-Ni is obviously more positive, indicating better corrosion resistance. Oliveira, Carlos and Lotfi all reported the co-deposition behavior of Zn-Ni electrodeposited coating [17-19]. It was found out that the initial deposition potential of Zn-Ni was round -1.15 V while the oxidation potential of Zn-Ni was around -0.33 V which was similar to the results found in the paper. The small difference between voltages may be due to the difference substrates and reference electrodes.

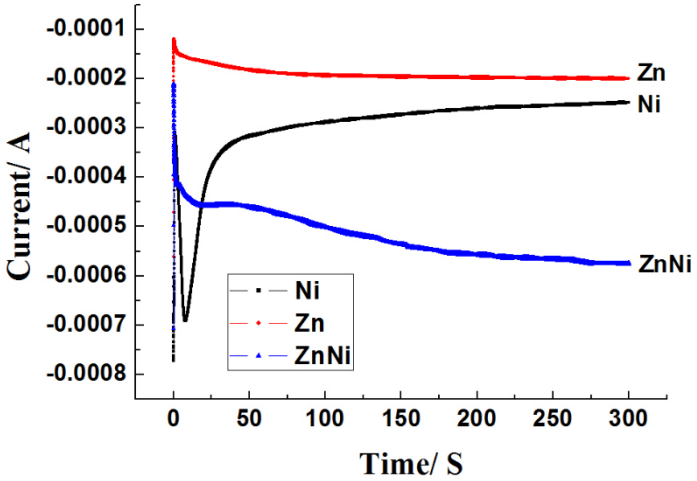

Figure 3. The chronoamperometry curves of 40Mn steel plate in different plating solutions containing 0.01 mol/L $NiCl_2$, 0.01 mol/L $ZnCl_2$ and 0.01 mol/L $NiCl_2$+$ZnCl_2$ respectively; The working electrode is 40Mn steel plate (1 cm×1 cm×0.1 cm) while the counter electrode is pure platinum plate (2 cm×2 cm×0.1 cm). The saturated calomel electrode is used as the reference electrode. The deposition potential keeps at -1.3 V for 5 min.

Figure 3 shows the chronoamperometry curves of Zn, Ni and Zn-Ni alloy at -1.3 V for 5 min. It is clear that the cathode current first decreases and then increases, and then reaches equilibrium. At the beginning of electrodeposition, the cathode current decreases due to the double layer charge. With the deposition process, the grains on the surface of the substrate nucleate and grow into particles, which increase the surface area of the coating resulting in the increase of the cathode current. When the deposition system reaches equilibrium, the cathode current is stable. Moreover, the deposition current of zinc is the smallest and that of Zn-Ni alloy is the largest after the electrodeposition gets equilibrium.

3.2 Composition and current efficiency of Zn-Ni coating

It has been found that the composition of nickel in Zn-Ni alloy directly affects the corrosion resistance of Zn-Ni alloy. Although according to the previous cyclic voltammetry analysis, nickel is easier to be electrodeposited than zinc. However, Zn-Ni alloy electrodeposition belongs to anomalous co-deposition [20-21]. In the actual electrodeposition process, the increase of pH value near the

cathode is more likely to generate zinc hydroxide and hinder the mass transfer process of nickel ion, thus reducing the content of nickel in the coating. According to the previous cyclic voltammetry curve, the deposition of nickel is controlled by electrochemistry. Therefore, increasing the current density of electrodeposition is beneficial to accelerate the deposition process of nickel and increase the content of nickel in the coating. This section mainly studies the effect of current density on the performances of Zn-Ni alloy.

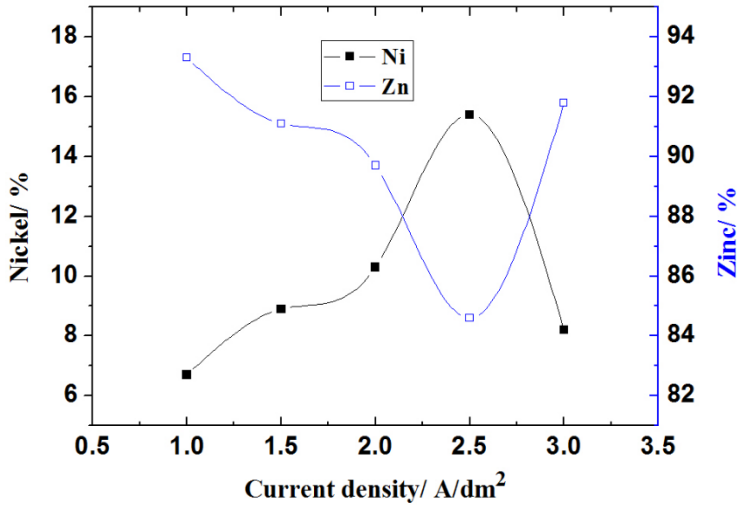

Figure 4. Effect of current density on composition of Zn-Ni coatings prepared using different current density: a. 1 A/dm^2; b. 1.5 A/dm^2; c. 2 A/dm^2; d. 2.5 A/dm^2; e. 3 A/dm^2; Energy resolution is 160±5 eV with 1 ppm precision.

The composition of Zn-Ni electrodeposited coatings prepared by different current densities is shown in figure 3. It is clear that the zinc content in Zn-Ni alloy coating is much higher than nickel content. Moreover, the amount of nickel in the Zn-Ni ally coating is much less than that of in the plating solution due to anomalous co-deposition. During the Zn-Ni electrodeposition process, hydrogen evolution near cathode results in the increase of pH value which attributes to the formation of $Zn(OH)_2$ colloid shown in equation 1.

$$Zn^{2+} + 2OH^- \Leftrightarrow Zn(OH)_2 \qquad (1)$$

The $Zn(OH)_2$ colloid adsorbed on the cathode surface allows the passage of zinc ions, but inhibits the transfer of nickel ions, thus decreasing the electrodeposition rate of nickel. The Zn-Ni coating obtained at the condition of 1 A/dm^2 has 93.3% zinc content, but only 6.7% nickel content. With the increase of current density, the amount of zinc in the coating decreases slowly while the nickel content increases gradually. When the current density is 2.5 A/dm^2, the nickel content in the Zn-Ni coating increases to 15.4 % which is almost three times larger than that of Zn-Ni coating obtained at the condition of 1 A/dm^2.

Because the electrodeposition of nickel is controlled by electrochemistry, increasing the current density is beneficial to accelerate the mass transfer rate of nickel, thus increasing the content of nickel in Zn-Ni coating. However, when the current density reaches 3 A/dm^2, the pH value of the cathode surface rises sharply due to the intense hydrogen evolution, and a large amount of nickel and zinc

hydroxide is precipitated, which hinders the deposition of nickel. Therefore, the content of nickel in the coating decreases sharply.

There are many side reactions in the electrodeposition process, such as hydrogen evolution, water electrolysis and so on. Therefore, the current efficiency of electrodeposition is less than 100%. If the current efficiency is too low, not only the energy waste is large, but also will lead to unstable plating solution. The current efficiency of Zn-Ni electrodeposited coating can be calculated by equation 2 and equation 3.

$$\eta = \frac{M_A}{M_T} \times 100\% = \frac{M_A}{K_{ZnNi} it} \times 100\% \qquad (2)$$

$$K_{ZnNi} = \frac{100}{\frac{P_{Zn}}{K_{Zn}} + \frac{P_{Ni}}{K_{Ni}}} \qquad (3)$$

Meanwhile, M_A is the actual mass deposition on the cathode, M_T is theoretical mass deposition on cathode, $K_{Zn\text{-}Ni}$ is electrochemical equivalent of Zn-Ni alloy coating, i is total current, t is the total electrodeposition time; P_{Zn} is percentage of zinc content on Zn-Ni alloy coating; P_{Ni} is percentage of nickel content on Zn-Ni alloy coating; K_{Zn} is electrochemical equivalent of Zn (1.220 $gA^{-1}h^{-1}$), K_{Ni} is electrochemical equivalent of Ni (1.095 g $A^{-1}h^{-1}$). The detail information of current efficiency calculated is listed in table 3.

Table 3. Current efficiency of Zn-Ni coatings prepared using different current density: a. 1 A/dm^2; b. 1.5 A/dm^2; c. 2 A/dm^2; d. 2.5 A/dm^2; e. 3 A/dm^2;

Current Density A/dm^2	**Ni/ %**	**Zn/ %**	**$K_{Zn\text{-}Ni}$ / $gA^{-1}h^{-1}$**	**M_A/ mg**	**M_T/ mg**	**Current efficiency/ %**
1	6.7 %	93.3 %	1.211	59.02	72.66	81.23
1.5	8.9 %	91.1 %	1.208	95.01	108.72	87.39
2	10.3 %	89.7 %	1.206	132.26	144.72	91.39
2.5	15.4 %	84.6 %	1.199	168.30	179.85	93.58
3	8.2 %	91.8 %	1.209	182.47	217.62	83.85

According to table 3, with the increase of current density, the current efficiency of Zn-Ni electrodeposited coating shows different trends. When the current density is 1 A/dm^2, due to the slow mass transfer rate of nickel, the zinc hydroxide produced near the cathode greatly hinders the deposition of nickel, so that the content of nickel in the coating is greatly reduced, resulting in lower current efficiency. As the electrodeposition of nickel is controlled by electrochemistry, with the increase of current density, the mass transfer and deposition rate of nickel are greatly improved, leading to the improve of the current efficiency. Nevertheless, when the current density is 3 A/dm^2, the intense hydrogen evolution reduces the deposition efficiency of Zn-Ni alloy coatings to a certain extent. In addition to current density, it has been reported that other parameters such as temperature, pH, etc also affect the current efficiency of electrodeposition [22-23].

3.3 Thickness of Zn-Ni coating

Figure 5 and table 4 show the influence of different current densities on the thickness of Zn-Ni coating. It is found out that thickness of Zn-Ni alloy prepared under different current densities is not the same. As the current density increases, the thickness of the Zn-Ni alloy coating increases from 7.3 μm to 23.4 μm and then decreases to 13.4 μm. According to the previous analysis, appropriately increasing the current density is beneficial to accelerate the mass transfer rate of nickel ion, improve the electrodeposition efficiency, and thus increase the thickness of the coating. However, when the current density increases to 3 A/dm^2, the coating thickness decreases to 13.4 μm. The excessive current density will strengthen the cathode polarization and promote the hydrogen evolution which is conducive to the decrease of current efficiency. Intense hydrogen evolution during electrodeposition has been reported that will decrease the current efficiency and affect the compactness of coating [24-25].

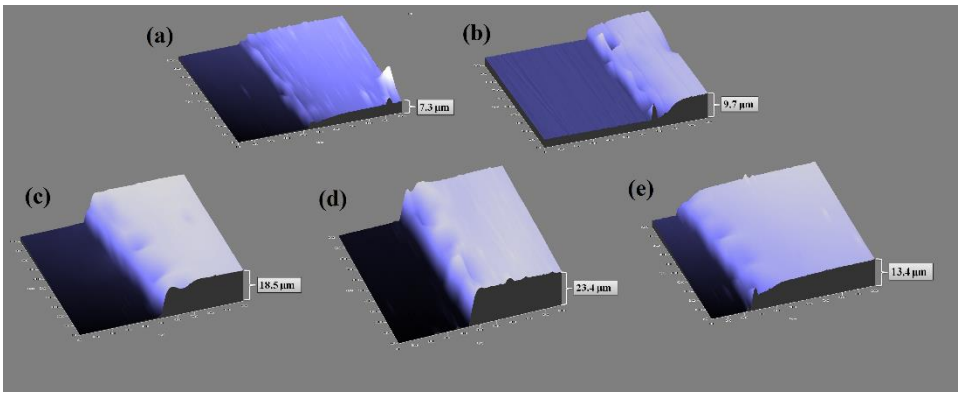

Figure 5. Effect of current density on thickness of Zn-Ni coatings prepared using different current density: a. 1 A/dm^2; b. 1.5 A/dm^2; c. 2 A/dm^2; d. 2.5 A/dm^2; e. 3 A/dm^2; The scanning length is 1000 μm with 10 μm/s scanning rate.

Table 4. Thickness of Zn-Ni coatings prepared using different current density: a. 1 A/dm^2; b. 1.5 A/dm^2; c. 2 A/dm^2; d. 2.5 A/dm^2; e. 3 A/dm^2; The scanning length is 1000 μm with 10 μm/s scanning rate.

Current Density A/dm^2	**Ni/ %**	**Zn/ %**	**Scanning length/ μm**	**Thickness/ μm**
1	6.7 %	93.3 %	1000	7.3
1.5	8.9 %	91.1 %	1000	9.7
2	10.3 %	89.7 %	1000	18.5
2.5	15.4 %	84.6 %	1000	23.4
3	8.2 %	91.8 %	1000	13.4

3.4 Corrosion resistance of Zn-Ni coating in simulated concrete pore solution

Surface morphology of Zn-Ni alloy coatings obtained by different current densities is shown in

figure 6. The surface of Zn-Ni alloy coating prepared with 1 A/dm^2 current density is rough and the porosity is high. With the increase of current density, strip particles are covered on the surface of Zn-Ni alloy coating. The surface particles of Zn-Ni alloy prepared at 2.5 A/dm^2 current density are compact with fewer cracks. The increase of current density is beneficial to increase the nickel content in the coating, and the nickel entering into the lattice and grain boundary of the alloy could refine the grains. When the current density is 3 A/dm^2, intense hydrogen evolution and a large amount of metal hydroxide adsorbed on the cathode surface resulting in the increase of roughness, cracks and pores.

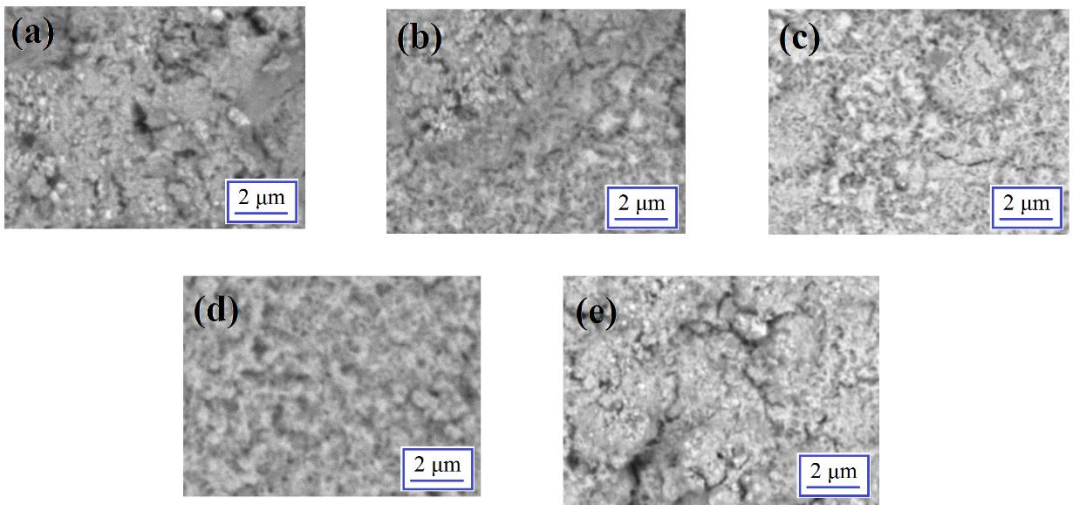

Figure 6. Effect of current density on surface morphology of Zn-Ni coatings prepared using different current density: a. 1 A/dm^2; b. 1.5 A/dm^2; c. 2 A/dm^2; d. 2.5 A/dm^2; e. 3 A/dm^2; The accelerating voltage is 15 kV with 8.2 mm working distance.

The polarization curves of Zn-Ni electrodeposited coatings are shown in figure 7. It can be seen that Zn-Ni coatings prepared by different current densities present different self corrosion potential and corrosion current density. Table 5 below lists the self potential and corrosion current density of Zn-Ni coatings.

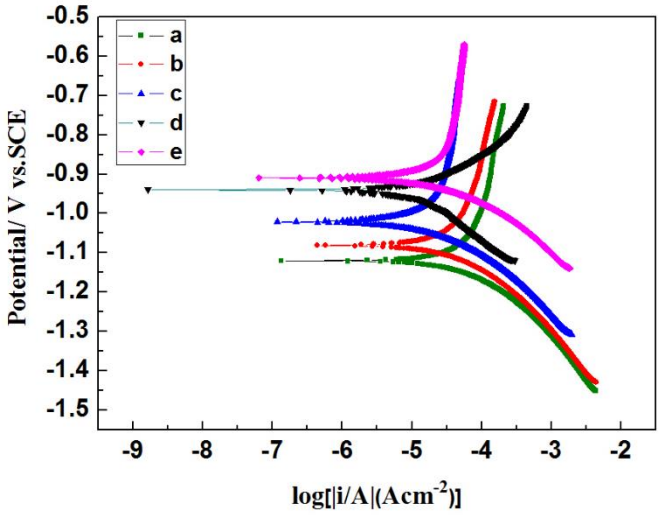

Figure 7. Polarization curve of Zn-Ni alloy coating prepared using different current density in simulated concrete pore solution: a. 1 A/dm^2; b. 1.5 A/dm^2; c. 2 A/dm^2; d. 2.5 A/dm^2; e. 3 A/dm^2; The working electrode is 40Mn steel plate (1 cm×1 cm×0.1 cm) while the counter electrode is pure platinum plate (2 cm×2 cm×0.1 cm). The saturated calomel electrode is used as the reference electrode. The scanning rate is 3 mV/s.

Table 5. E_{corr} and J_{corr} of Zn-Ni coatings prepared using different current density in simulated concrete pore solution: a. 1 A/dm^2; b. 1.5 A/dm^2; c. 2 A/dm^2; d. 2.5 A/dm^2; e. 3 A/dm^2; The working electrode is 40Mn steel plate (1 cm×1 cm×0.1 cm) while the counter electrode is pure platinum plate (2 cm×2 cm×0.1 cm). The saturated calomel electrode is used as the reference electrode. The scanning rate is 3 mV/s.

Current Density A/dm^2	Ni/ %	Zn/ %	E_{corr}/ V	J_{corr}/ μA
1	6.7 %	93.3 %	-1.121	53.4
1.5	8.9 %	91.1 %	-1.084	32.7
2	10.3 %	89.7 %	-1.019	18.5
2.5	15.4 %	84.6 %	-0.942	8.7
3	8.2 %	91.8 %	-0.907	21.3

It is obvious that, with the increase of current density, the self corrosion potential of Zn-Ni alloy gradually moves positively. When the current density increases from 1 A/dm^2 to 3 A/dm^2, the self corrosion potential of Zn-Ni alloy coating moves to more positive position from -1.12 V to -0.91 V. The positive shift of the self corrosion potential of the Zn-Ni coating is due to the increase of the content of nickel and nickel hydroxide in the coating. At the condition of 2.5 A/dm^2 current density, the Zn-Ni alloy coating prepared has the lowest current density and the best corrosion resistance. The corrosion mechanism of Zn-Ni alloy is listed in equations below [26-27].

$$Zn - 2e \rightarrow Zn^{2+} \quad (4)$$

$$Zn^{2+} + 2H_2O \rightarrow Zn(OH)_2 + 2H^+ \quad (5)$$

$$Zn(OH)_2 \rightarrow ZnO + H_2O \qquad (6)$$

The zinc in the Zn-Ni alloy coating is oxidized to zinc ions, and zinc hydroxide is generated in an aqueous solution or alkaline environment. Since the zinc hydroxide is not very stable, it will be converted to zinc oxide. Because zinc oxide is a semiconductor material with loose structure, the corrosion resistance performance is poor. With the increase of nickel content in Zn-Ni alloy, nickel can inhibit the formation of zinc oxide, which is beneficial to improve the corrosion resistance. It is reported that the main corrosion products of Zn-Ni alloy are zinc chloride and zinc hydroxide [28-30].

4. CONCLUSIONS

In this paper, Zn-Ni alloy is prepared by electrodeposition technology. The effects of different current densities on the electrochemical process, composition, thickness, surface morphology and corrosion resistance of Zn-Ni alloy are studied. It is found that electrodeposition of Zn-Ni alloy is a typical anomalous co-deposition phenomenon. The zinc ions in the plating solution will hinder the electrodeposition of nickel, and the content of nickel in the coating will be reduced. The increase of current density is beneficial to accelerate the mass transfer and deposition rate of nickel, thus increasing the content of nickel in Zn-Ni coating. The Zn-Ni alloy coating prepared at 2.5 A/dm^2 current density possesses a nickel content of 15.4% and has a compact surface morphology with the best corrosion resistance.

References

1. J. K. Ren, D. S. Mao, Y. Gao, J. Chen and Z. Y. Liu, *Mater. Sci. Eng., A*, 827 (2021) 141959.
2. T. He, W. Emori, R. H. Zhang, P. C. Okafor, M. Yang and C. R. Cheng, *Bioelectrochem*., 130 (2019) 107332.
3. R. Hossain, F. Pahlevani and V. Sahajwalla, *Mater. Charact*., 148 (2019) 116.
4. R. C. Saxena, J. Biswal, H. J. Pant, J. S. Samantray, S. C. Sharma, A. K. Gupta and S. S. Ray, *Appl. Radiat. Isot*., 135 (2018) 201.
5. A. Medjaldi, A. Himour, M. Bououdina, S. Ouchenane and A. Gharbi, *Metall. Microstruct. Anal*., 10 (2021) 208.
6. H. Li, S. R. Yu, X. X. Han, S. B. Zhang and Y. Zhao, *J. Bionic Eng*., 13 (2016) 622.
7. O. O. Oluwole, D. T. Oloruntoba and O. Awheme, *Mater. Des*., 29 (2008) 1266.
8. N. M. Chavan, B. Kiran, A. Jyothirmayi, P. S. Phani and G. Sundararajan, *J. Therm. Spray Technol*., 22 (2013) 463.
9. Y. D. Yu, X. X. Zhao, M. G. Li, G. Y. Wei, L. X. Sun and Y. Fu, *Surf. Eng*., 29 (2013) 743.
10. S. Arora, B. Sharma and C. Srivastava, *Surf. Coat. Technol*., 398 (2020) 126083.
11. M. K. P. Kumar, M. Y. Rekha, J. Agrawal, T. M. Agarwal and C. Srivastava, *J. Alloys Compd*., 783 (2019) 820.
12. M. Moshtaghi, M. Safyari and G. Mori, *Electrochem. Commun*., 134 (2022) 107169.
13. C. Muller, M. Sarret and E. Garcia, *Electrochem. Commun*., 47 (2005) 307.
14. X. P. Qiao, H. L. Li, W. Z. Zhao and D. J. Li, *Electrochim. Acta*, 89 (2013) 771.
15. R. Q. Li, Q. J. Dong, J. Xia, C. H. Luo, L. Q. Sheng, F. Cheng and J. Liang, *Surf. Coat. Technol*., 366 (2019) 138.
16. Y. D. Yu, Y. Cao, M. G. Li, G. Y. Wei and H. Dettinger, *Mater. Res. Innovations*, 18 (2014) 314.

17. E. M. D. Oliveira, W. Rubin and I. A. Carlos, *J. Appl. Electrochem*., 39 (2009) 1313.
18. E. M. D. Oliveira and I. A. Carlos, *Surf. Coat. Technol*., 206 (2011) 250.
19. N. Lotfi, M. Aliofkhazraei, H. Rahmani and G. B. Darband, *Prot. Met. Phys. Chem*., 54 (2018) 1102.
20. S. L. Diaz, O. R. Mattos, O. E. Barcia and F. J. F. Miranda, *Electrochim. Acta*, 47 (2002) 4091.
21. C. Srivastava, S. K. Ghosh, S. Rajak, A. K. Sahu, R. Tewari, V. Kain and G. K. Dey, *Surf. Coat. Technol*., 313 (2017) 8.
22. C. Srivastava, S. K. Ghosh, S. Rajak, A. K. Sahu, R. Tewari, V. Kain and G. K. Dey, *Surf. Coat. Technol*., 313 (2017) 8.
23. I. Tabakovic, S. Riemer, N. Jayaraju, V. Venkatasamy and J. Gong, *Electrochim. Acta*, 58 (2011) 25.
24. Y. Y. Wang, H. J. Xiao and L. Y. Chai, *J. Cent. South Univ*., 15 (2008) 814.
25. V. S. Nikitin, T. N. Ostanina, V. M. Rudoi, T. S. Kuloshvili and A. B. Darintseva, *J. Electroanal. Chem*., 870 (2020) 114230.
26. M. Y. Rekha and C. Srivastava, *Metall. Mater. Trans. A*, 50 (2019) 5896.
27. A. R. E. Sayed, H. S. Mohran and H. M. A. E. Lateef, *Metall. Mater. Trans. A*, 43 (2012) 619.
28. H. M. A. E. Lateef, A. R. E. Sayed and H. S. Mohran, *T. Nonferr. Metal. Soc*., 25 (2015) 2807.
29. M .Kowalski and A. Stachowiak, *Surf. Coat. Technol*., 366 (2019) 75.
30. R. Gnanamuthu, S. Mohan, G. Saravanan and C. W. Lee, *J. Alloys Compd*., 513 (2012) 449.